

# Low-Shrinkage, High-Hardness, and Transparent Hybrid Coatings: Poly(methyl methacrylate) Cross-Linked with Silsesquioxane

John H. Harreld,<sup>\*,†</sup> Akira Esaki,<sup>‡</sup> and Galen D. Stucky<sup>†</sup>

Department of Chemistry and Biochemistry, University of California, Santa Barbara, Santa Barbara, California 93106, and Precision Coating and Surface Modification Laboratory, MCC-Group Science and Technology Research Center, Mitsubishi Chemical Corporation, Research Center, 1000, Kamoshida-cho, Aoba-ku, Yokohama 227-8502, Japan

Received January 28, 2003

Copolymers of trimethoxysilylpropyl methacrylate (TMSPM) and methyl methacrylate (MMA) with varied composition and molecular weight were prepared as building blocks for transparent organic–inorganic hybrid materials. Thermally and chemically induced condensation of these network precursors after solvent evaporation results in optically clear coatings as thick as 1.0 mm with extremely low lateral shrinkage. Many interacting variables such as acid catalyst concentration, polymer molecular weight, polymer composition, and thermal treatment combine to produce materials having controllable shrinkage, hardness, transparency, and thermal stability. By selectively defining these variables, the syntheses of these materials are optimized such that silsesquioxane-cross-linked acrylic polymers are produced that exhibit desirable properties such as low optical loss in the visible spectrum, low lateral shrinkage, high scratch hardness, and no glass transition temperature. The available combinations, interrelationships, and limitations of these properties are discussed.

## Introduction

The sol–gel approach has been demonstrated to be a highly effective synthesis method to design and create many new types of inorganic–organic hybrid materials, and this topic has been the subject of several reviews<sup>1</sup> and special issues<sup>2</sup> in the literature. The low-temperature solution conditions of sol–gel processing make possible nanoscale mixing of inorganic and organic components that can be precursors to hybrid solids. By this approach, multifunctional materials with homogeneous microstructures may be designed and synthesized which have an extensive range of mechanical, chemical, optical, and electronic properties.

Many optical applications such as lenses, coatings, and display substrates require materials with high transparency in the visible spectrum. Even when two highly transparent phases such as silica glass and acrylic polymer are mixed, optical losses from scattering will arise in these materials if these phases separate into domains greater than tens of nanometers.<sup>3–6</sup> Several methods of obtaining such hybrid structures with-

out phase separation were investigated in previous related work on poly(methyl methacrylate) modified silicate xerogels based on tetramethoxysilane (TMOS), methyl methacrylate (MMA), and the cross-linking agent trimethoxysilylpropyl methacrylate (TMSPM).<sup>7</sup> The most successful method involved dissolving the sol components in a common solvent before inducing sequential polymerization treatments in which the organic network was fully formed before condensation of the inorganic groups. Also from this work, the use of a single molecule hybrid precursor TMSPM was determined to result in high-quality hybrid optical materials.

A significant amount of work has been published in which such a hybrid precursor is used to create inorganic–organic hybrid materials. Especially representative of this area is the research from the groups of Schmidt<sup>8</sup> and Seddon.<sup>9</sup> The majority of hybrid IPN materials reported in the literature are made following the same general strategy, which is focused on traditional sol–gel chemistry. By this approach, the formation of an inorganic resin network into a gel or resin precedes later cross-linking by UV or thermally polymerizable organic monomer or covalently bound functional group. The formation of inorganic gels often results in greater than 50% volume shrinkage from

\* Corresponding author. E-mail: jharreld@chem.ucsb.edu.

<sup>†</sup> University of California.

<sup>‡</sup> Mitsubishi Chemical Corporation.

(1) See, for examples, (a) Sanchez, C.; Ribot, F. *New J. Chem.* **1994**, 18, 1007. (b) Schubert, U.; Husing, N.; Lorenz, A. *Chem. Mater.* **1996**, 7, 2010. (c) Wen, J.; Wilkes, G. L. *Chem. Mater.* **1996**, 8, 1667. (d) Judeinstein, P.; Sanchez, C. *J. Mater. Chem.* **1996**, 6, 511. (e) Corriu, R. J.; Leclercq, D. *Angew. Chem., Int. Ed. Engl.* **1996**, 35, 1420. (f) Sanchez, C.; Soler-Illia, G. J. A. A.; Ribot, F.; Lalot, T.; Mayer, C. R.; Cabuil, V. *Chem. Mater.* **2001**, 13, 3061.

(2) See, for examples, (a) "Organic–Inorganic Nanocomposite Materials," special issue of *Chem. Mater.* **2001**, 13, 3059–3809. (b) "Hybrid Organic–Inorganic Materials," special issue of *MRS Bull.* **2001**, 26, 356–424.

(3) Landry, C. J. T.; Coltrain, B. K.; Brady, B. K. *Polymer* **1992**, 33, 1486.

(4) Coltrain, B. K.; Landry, C. J. T.; O'Reilly, J. M.; Chamberlain, A. M.; Rakes, G. A.; Sedita, J. S.; Kelts, L. W.; Landry, M. R.; Long, V. K. *Chem. Mater.* **1993**, 5, 1445.

(5) Jackson, C. L.; Bauer, B. J.; Nakatani, A. I.; Barnes, J. D. *Chem. Mater.* **1996**, 8, 727.

(6) Huang, Z. H.; Qui, K. Y. *Polymer* **1997**, 38, 521.

(7) Harreld, J. H.; Dunn, B.; Zink, J. I. *J. Mater. Chem.* **1997**, 7, 1511.

syneresis and capillary stresses during solvent evaporation.<sup>10</sup> For many applications, such as optical coatings, only a very low amount of lateral shrinkage (ca. 0–3%) is acceptable. Organically cross-linked resins may be cast into shape and cured with considerably lower shrinkage, but in these materials the low mobility of anchored vinyl groups is more likely to result in an organic network composed of oligomer instead of polymer.

An alternative synthesis approach to hybrid IPNs ("inorganic–organic" materials) is available by reversing the sequence of network formation. It is known that the sequence of network formation greatly effects the properties of the prepolymer intermediate<sup>11</sup> and the cross-linked IPN<sup>7</sup> of single-component TMSPM-based hybrid materials. Thus, compositionally similar but structurally unique hybrid IPNs ("organic–inorganic" materials) are obtained in which acrylic polymers are cross-linked by inorganic linkages. The development of this strategy is primarily due to Wei and co-workers.<sup>12</sup> In all but relatively few cases<sup>13</sup> these investigations have been limited to systems in which an additional inorganic cross-linking agent such as tetraethoxysilane (TEOS) is added to the organic polymeric precursor to increase the degree of cross-linking and the total silica content.

We anticipate several advantages that may derive from instead cross-linking the organic network with only the minimum of inorganic content needed to obtain the desired enhancement in physical properties. For example, higher-toughness and lighter-weight materials may be produced. Additionally, the tendencies for shrinkage after inorganic gel formation and for light scattering due to phase separation are expected to decrease considerably.

In the present work, the concentration and the reaction kinetics of trialkoxysilane cross-linking sites in TMSPM-based polymers and TMSPM–MMA based copolymers are systematically varied to create highly transparent, thick coatings of poly(methyl methacryl-

ate)/polysilsesquioxane IPN. These materials exhibit extremely low shrinkage and improved heat resistance and mechanical properties when compared with those of conventional optical plastics. The effects of polymer composition, molecular weight, condensation chemistry, and curing treatments on the assembly, network structure, and material properties are presented and discussed to provide material design and synthesis guidelines.

## Experimental Methods

Acrylic polymers and copolymers of TMSPM (Aldrich) and MMA (Aldrich, deinhibited through column) were prepared at concentrations between 25 and 30 wt % using tetrahydrofuran (THF) as the solvent. Photopolymerization of the acrylates was initiated by azobisisobutyronitrile (AIBN, Aldrich) under 365-nm irradiation from an 8-W UV lamp. The ratio of initiator to monomer was varied by orders of magnitude between 1:10 and 1:1 000 000. Cross-linked samples were prepared by HCl catalyzed hydrolysis of the alkoxy silane groups in THF/polymer solutions. The concentration of acid was varied, but a water/silane ratio of 3:1 was held constant unless otherwise noted. Thick films were made by casting acidified polymer solutions into glass containers (2.5 cm diam) and allowing them to dry under ambient conditions. The drying procedure was performed in air and involved at least 12 h at 80 °C (after heating at 2 °C/min) followed by 3 h at 100 °C (after heating at 1 °C/min). Selected dry films were then cured at either 150 or 200 °C in air for an additional 3 h (heating and cooling rates were equal to and less than 1 °C/min, respectively).

Molecular weight distribution (MWD), polydispersity index (PDI), and Mark–Houwink parameter ( $a_{MH}$ ) data from polymeric products were obtained by triple-detection gel permeation chromatography (GPC) measurements. The triple-detection GPC system employed included a Waters Alliance 2690 separation module equipped with a Waters 2410 differential refractometer and a Viscotek T60A dual detection system with differential viscosimetry and laser light scattering detectors. The size-exclusion gel column set consisted of a PLgel 5- $\mu$ m Guard and two PLgel 5- $\mu$ m Mixed-C columns (Polymer Laboratories, linear range from 200 to 2 000 000 amu) arranged in series. Detector calibration, data acquisition, and data processing were performed through the Viscotek TriSEC software package. Samples for GPC characterization were prepared by diluting solutions of polymer product into THF to concentrations of approximately 10 wt % and filtering the solution through a 0.2- $\mu$ m polypropylene filter. Sample volumes of 100  $\mu$ L were measured at 30 °C and in THF flowing at 1.00 mL/min. Polystyrene standards with molecular mass of 90 100 amu (Viscotek) were measured at the beginning of each sample set to calibrate the light-scattering detector.

Solid state <sup>29</sup>Si NMR samples were measured in a 4-mm zirconia rotor spinning at 10 kHz using a silicon-free probe and a Bruker AVANCE 500 MHz spectrometer. A single 30° RF pulse was applied on the <sup>29</sup>Si channel with a 45-s pulse delay and a proton decoupling composite pulse. Solution <sup>29</sup>Si NMR samples were measured from d-THF solutions in a 10-mm glass tube spinning at 20 Hz and using an 8-s pulse delay. The sample solutions also contained a 0.02 M concentration of chromium tris(acetylacetonate) as a spin relaxing agent. All <sup>29</sup>Si shifts are referenced to tetramethylsilane (TMS). Chemical shifts of silicon atoms in silsesquioxane compounds are referred to using the traditional terminology  $T^n$  where the superscript corresponds to the number of oxygen bridges to other silicon atoms. Thus, an uncondensed monomer is designated  $T^0$ , and a fully condensed network with no residual silanols would be composed of  $T^3$  silicon atoms. The assignment of silsesquioxane structural components with <sup>29</sup>Si chemical shifts is in agreement with the literature.<sup>13,14</sup> Infrared absorp-

(8) (a) Nass, R.; Arpac, E.; Glaubitt, W.; Schmidt, H. *J. Non-Cryst. Solids* **1990**, *121*, 370. (b) Schmidt, H.; Popall, M. *Proc. SPIE* **1990**, *1328* (Sol–Gel Optics), 249. (c) Popall, M.; Meyer, H.; Schmidt, H.; Schulz, J. *Mater. Res. Soc. Symp. Proc.* **1990**, *180* (Better Ceramics for Chemistry IV), 995. (d) Schmidt, H.; Krug, H.; Kasemann, R.; Tiefensee, F. *Proc. SPIE* **1991**, *1590* (Submolecular Glass Chemical Physics), 36. (e) Krug, H.; Merl, N.; Schmidt, H. *J. Non-Cryst. Solids* **1992**, *147*–148, 447. (f) Schmidt, H. *Ceram. Trans.* **1995**, *55*, 307. (g) Muller, P.; Braune, B.; Becker, C.; Krug, H.; Schmidt, H. *Proc. SPIE* **1997**, *3136* (Sol–Gel Optics IV), 462. (h) Muller, P.; Becker, C.; Schmidt, H. *Mater. Res. Soc. Symp. Proc.* **1998**, *519* (Organic/Inorganic Hybrid Materials), 995.

(9) (a) Lana, S. L.; Seddon, A. B. *Ceramica (Sao Paulo)* **1996**, *42*, 650. (b) Seddon, A. B.; Adamjee, A. *Proc. SPIE* **1998**, *3469* (Organic–Inorganic Materials for Photonics), 108. (c) Tadanaga, K.; Ellis, B.; Seddon, A. B. *J. Sol-Gel Sci. Technol.* **2000**, *19*, 687.

(10) Yoldas, B. E. *J. Mater. Sci.* **1986**, *21*, 1087.

(11) Bersani, D.; Lottici, P. P.; Tosini, L.; Montenero, A. *J. Raman Spectrosc.* **1999**, *30*, 1043.

(12) (a) Wei, Y.; Bakthavatchalam, R.; Whitecar, C. K. *Chem. Mater.* **1990**, *2*, 337. (b) Wei, Y.; Yang, D.; Bakthavatchalam, R. *Mater. Lett.* **1992**, *13*, 261. (c) Wei, Y.; Wang, W.; Yeh, J.-M.; Wang, B.; Yang, D.; Murray, J. K., Jr. *Adv. Mater.* **1994**, *6*, 372. (d) Xu, C.; Eldada, L.; Wu, C.; Norwood, R. A.; Shacklette, L. W.; Yardley, J. T.; Wei, Y. *Chem. Mater.* **1996**, *8*, 2701. (e) Wei, Y.; Jin, D.; Yang, C. *J. Sol-Gel Sci. Technol.* **1996**, *7*, 191. (f) Wei, Y.; Jin, D.; Yang, C.; Wei, G. *Polym. Mater. Sci. Eng.* **1996**, *74*, 244. (g) Wei, Y.; Jin, D.; Yang, C.; Kels, M. C.; Qui, K.-Y. *Mater. Sci. Eng. C*, **1998**, *6*, 91. (h) Wei, Y.; Jin, D.; Wei, G.; Yang, D.; Xu, J. *J. Appl. Polym. Sci.* **1998**, *70*, 1689. (i) Wei, Y.; Feng, Q.; Xu, J.; Dong, H.; Qui, K.-Y.; Jansen, S. A.; Yin, R.; Ong, K. A. *Adv. Mater.* **2000**, *12*, 1448.

(13) Furukawa, H.; Kato, Y.; Ando, N.; Inoue, M.; Lee, Y. K.; Hazan, I.; Omura, H. *Prog. Org. Coatings* **1994**, *24*, 81.

(14) Nishiyama, N.; K. Horie, K. *J. Appl. Polym. Sci.* **1987**, *34*, 1619.

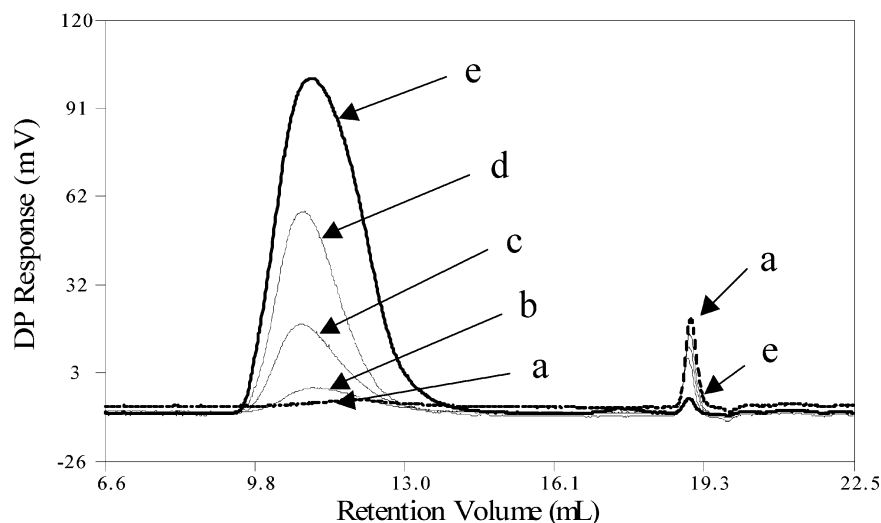


**Figure 1.** GPC data from viscosimetry detector for TMSPM homopolymer samples prepared using UV exposure of (a) 1, (b) 3, (c) 7, (d) 14, and (e) 96 h; ratio of initiator/monomer = 1:10 000.

**Table 1. Gelation Times for TMSPM Homopolymer in the Presence of Residual TMSPM Monomer**

monomer conversion (%)	gelation time <sup>a</sup> (min)
0	$> 2 \times 10^4$
6	$> 2 \times 10^4$
20	18
60	8

<sup>a</sup>In each case the total concentration of acrylate units and HCl is the same.

tion spectra of samples dispersed in KBr pellets were measured in transmission using a Nicolet Magna 850 IR spectrometer.

Thermogravimetric analyses (TGA) and differential thermal analyses (DTA) were performed on finely ground samples using a Netzsch STA 409 simultaneous thermal analyzer in air between room temperature and 1000 °C at a heating rate of 2 °C/min. Scratch hardness measurements were made on thick film samples according to ASTM designation D3363 using a range of pencil hardness from 9B to 9H. UV-vis transmission data were recorded from dried and cured films on Pyrex substrates in the range of 280–800 nm using a Cary-14 spectrophotometer.

## Results

**1. Precursor Preparation.** Polymers of TMSPM and copolymers of TMSPM and MMA were synthesized in THF using UV treatments with AIBN as the free radical initiator. Raw data from GPC analyses were used to estimate the relative degree of monomer conversion by comparing the relative intensities of the polymer and monomer peaks (Figure 1). This index served as a tool to help define the effect that residual monomer has on the assembly of the network in terms of kinetics and hybrid structure. For example, a dramatic dependency of gelation time on the completeness of acrylate conversion is shown in Table 1. This is consistent with the observation that gelation times are much slower for low  $M_w$  polymer solutions compared to higher  $M_w$  polymer solutions of the same overall composition, concentration, and acid content (Figure 2). That is, larger polymeric precursors in random coil conformation are closer to spanning the sol volume than are smaller polymeric or oligomeric building blocks.

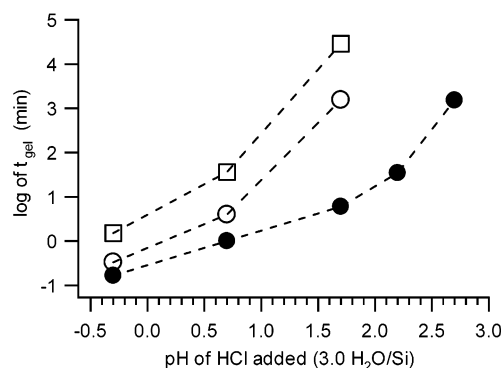


**Figure 2.** Relationship between gelation time (in sealed vials at 25 wt % in THF) and HCl concentration for homopolymer (1:0 TMSPM/MMA) of high  $M_w$  (280 000 amu, closed circles) and low  $M_w$  (9100 amu, open circles) and for copolymer (1:2 TMSPM/MMA) of low  $M_w$  (9700 amu, open squares).

There is another important difference between using an organic polymer precursor to synthesize organic–inorganic hybrid materials instead of the more traditional inorganic resin-based sol–gel approaches, specifically when residual monomer is present. If a significant fraction of residual monomer is present in a gelling solution of polymer, a portion of the monomer may react with the polymer and inhibit intermolecular siloxane condensation (i.e., cross-linking) with other polymer chains (Figure 3). An extreme case is that of the ORMOCER and NANOMER synthesis approaches in which no organic pre-polymerization is used.<sup>8,9</sup> In this case UV-induced organic cross-linking is the curing step. Thus, the final product (Figure 3, top) will be expected to have a very different network structure and resultant properties compared with those from pre-polymerization methods<sup>7,13</sup> (Figure 3, bottom).

To ensure independent control of the formation of each constituent network, siloxane polycondensation must not be induced by the conditions that promote complete vinyl polymerization. This emphasizes the importance of first distilling the THF to remove adsorbed water. It is known from <sup>29</sup>Si NMR analyses of polymer solutions having greater than 90% monomer conversion that the silane functional groups remain uncondensed during organic polymer formation (Figure



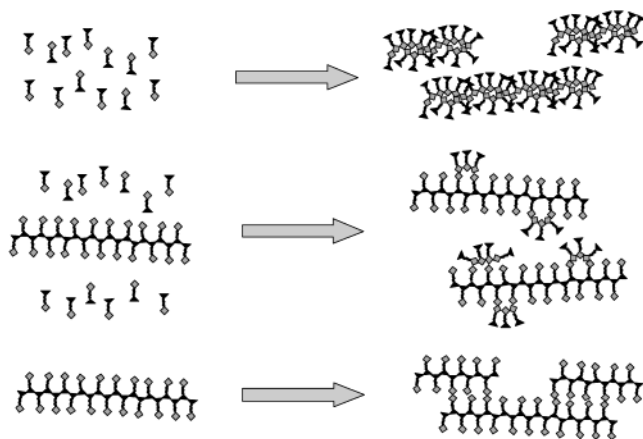


**Figure 3.** Schematic illustration of three types of hybrid organic-inorganic IPN assembly using TMSPM as the building block (gray diamonds represent the silane component, and black triangles represent the acrylic component). The top pathway presents the traditional sol-gel approach in which inorganic condensation is induced first and the resulting organically terminated resin is UV-cured to make a continuous network. The middle pathway occurs when acrylic monomer and polymer are mixed, as in the case of incomplete photopolymerization. In this case, formerly monomeric units block potential inorganic cross-linking sites such that intermolecular polymer network formation is inhibited. The bottom pathway illustrates our approach to induce inorganic condensation between fully polymerized acrylic units and form a highly cross-linked and unique IPN material.

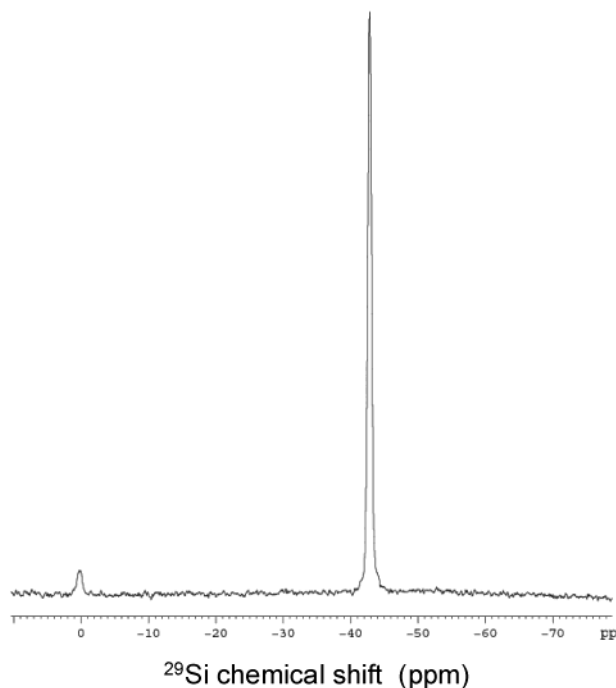


**Figure 4.** Solution  $^{29}\text{Si}$  NMR data from TMSPM homopolymer synthesized using an initiator/monomer ratio of 1:10 and UV irradiated for 48 h.

4). Moreover, polymer films cast from UV photopolymerized solutions without the addition of acid catalyst remain soluble in THF unless films are cured by successive thermal treatments.

Values of  $M_w$  from the processed GPC data (Figure 5) indicate that ratios of initiator/monomer between 1:10 and 1:10 000 are extremely effective in controlling the degree of polymerization, and furthermore that this

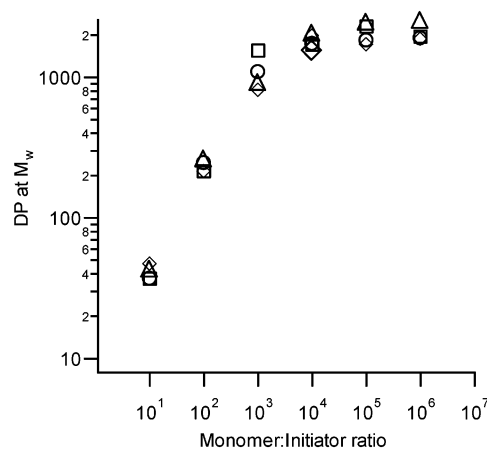


**Figure 5.** Degree of polymerization at the  $M_w$  as a function of the monomer/initiator ratio for polymer compositions of 1:0 (circles), 1:1 (squares), 1:3 (triangles), and 0:1 (diamonds) TMSPM/MMA.

**Table 2.** GPC Data from TMSPM-MMA Copolymer Solutions

TMSPM/MMA	AIBN/Monomer	$M_w$ (amu)	$DP_w^a$ (mer)	PDI <sup>b</sup>	$a_{MH}^c$
1:0	1:10	18 000	71	1.7	0.83
	1:1000	260 000	1000	1.5	0.87
1:1	1:10	17 000	97	1.7	0.85
	1:1000	220 000	1200	1.4	0.87
1:2	1:10	16 000	110	1.8	0.85
	1:1000	190 000	1200	1.4	0.88
1:4	1:10	20 000	160	2.1	0.87
	1:1000	190 000	1500	1.4	0.87

<sup>a</sup>  $DP_w$ , Degree of polymerization at  $M_w$ . <sup>b</sup> PDI, Polydispersity index. <sup>c</sup>  $a_{MH}$ , Mark-Houwink parameter.

level of control is general over each of the polymer compositions measured. A summary of the GPC results obtained from relatively high and low  $M_w$  polymers composed of 1:0, 1:1, 1:2, and 1:4 TMSPM/MMA is presented in Table 2. The duration of UV-irradiation resulting in at least 90% acrylate conversion using initiator/monomer ratios of 1:10 and 1:1000 was found to be 48 h and 7 days, respectively. Initiator-to-monomer ratios greater than 1:10 000 do not appear to be effective in producing significantly higher molecular weight polymers under these conditions.

**2. Network Formation.** Several studies were performed to define the gelation characteristics of the polymeric precursors into cross-linked xerogel and film products. Gelation time of polymer solutions in sealed vials was used as a relative measure of condensation kinetics. The data in Figure 6 are representative of the high sensitivity of condensation kinetics on both the water-to-silane ratio, homopolymer concentration, and acid concentration.

The rate of gelation of the polymer network must be carefully matched with the rate of solvent evaporation in order to obtain cross-linked and low-shrinkage films. When gelation occurs, the aspect ratio of the sample is effectively fixed. Adhesive forces between the film and the substrate coupled with compliance in the film network can allow some further loss of residual solvent without inducing lateral shrinkage; however, the bulk of the initial solvent content should be evaporated prior to gelation. If gelation is too slow, due to incomplete hydrolysis for example, then inorganic cross-linking might not occur at all. Therefore, a maximum sol-gel

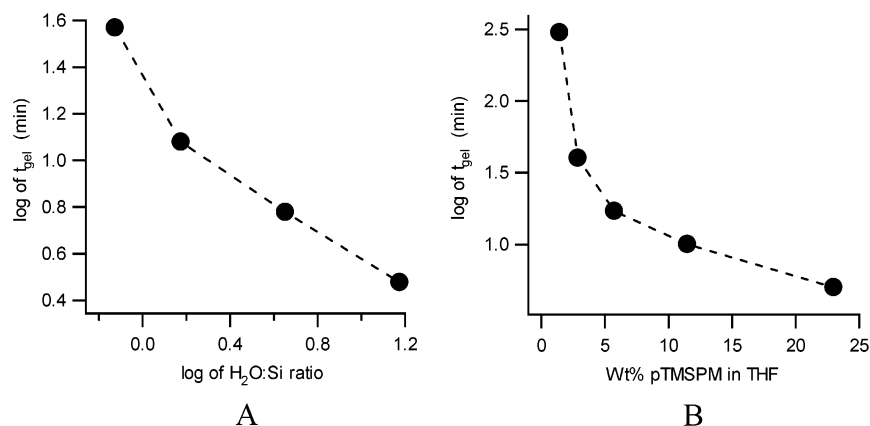


**Figure 6.** Dependency of TMSPM homopolymer gelation rate on (A)  $H_2O/Si$  ratio for a 23 wt % solution in THF using 0.020 N HCl, and (B) polymer concentration in THF using a 9:1 ratio of  $H_2O/Si$  and 0.020 N HCl; the homopolymer was synthesized using a ratio of 1:100.

**Table 3. Si NMR, Hardness, and DTA Data from Solvent-Cast, Thick ( $\sim 0.8$  mm) Films from Cross-Linked Homopolymer (10:1, Monomer/Initiator)**

pH of acid added (N)	$T_{cure}$ ( $^{\circ}C$ )	$T^0$ (mol. %)	$T^1$ (mol. %)	$T^2$ (mol. %)	$T^3$ (mol. %)	total degree of condensation (%)	HP <sup>a</sup>	$T_g^b$ ( $^{\circ}C$ )
1.7	100	26	32	38	4	40	2B	145
1.7	150	20	23	43	14	50	B	none
1.0	100	0	15	76	9	65	6H	140

<sup>a</sup> HP, Pencil hardness. <sup>b</sup>  $T_g$ , Glass transition temperature.

**Table 4. Si NMR and Hardness Data from Solvent-Cast, Thick ( $\sim 0.8$  mm) Films from Cross-Linked Copolymer (1:4 TMSPM/MMA, 20 k amu)**

pH of acid added (N)	$T_{cure}$ ( $^{\circ}C$ )	$T^0$ (mol. %)	$T^1$ (mol. %)	$T^2$ (mol. %)	$T^3$ (mol. %)	degree of condensation (%)	HP <sup>a</sup>
2.0	150	64	22	14	0	17	4H
2.0	200	28	39	22	11	39	7H

<sup>a</sup> HP, pencil hardness.

polycondensation rate is desired which also does not cause the material to gel prematurely. We also illustrated how the kinetics of sol-gel polycondensation in these systems are dependent on the polymer concentration in solution, the water-to-silane ratio, and the pH of the water added. The polymer concentration cannot be effectively set because it varies continuously during solvent evaporation, and the water-to-silane ratio is fixed at 3.0 so that complete hydrolysis of alkoxy-silanes may be achieved without excess water (which could promote partitioning and phase separation in THF). The remaining parameter, which can be easily controlled, is the pH of the HCl acid added to the polymer solution. As discussed, the composition and molecular weight of the selected polymer also play a role in determining the critical gelation times for a given acid concentration (Figure 2).

**3. Properties of Cured Materials.** Two general mechanisms of creating inorganic cross-links between acrylic polymers were investigated to determine the differences in network structure and resulting material properties arising from each. The first method is using a low concentration of acid catalyst to hydrolyze the alkoxy-silane groups and relying on thermal curing treatments for most of the condensative cross-linking. The second method is to use a higher concentration of acid catalyst so that a significantly greater amount of condensation has already occurred by the time the solvent has evaporated. To compare the resulting differences in structure and properties, and to identify

potential advantages of one approach over the other, representative materials were processed and characterized.

To represent the first case, a low  $M_w$  homopolymer (from a monomer/initiator ratio of 10:1) solution was hydrolyzed with 0.020 N HCl, solvent cast at room temperature, and dried at 100  $^{\circ}C$ . The resulting material ( $\sim 0.8$ -mm thick) exhibited 40% degree of siloxane condensation (Figure 7A), a pencil hardness of 2B, and a lateral shrinkage between 5 and 10% (Table 3). After curing at 150  $^{\circ}C$ , an identical film was cross-linked further to a 50% degree of siloxane condensation (Figure 7B) and a pencil hardness of B. No significant additional shrinkage was observed.

For comparison, the second cross-linking strategy is represented by the same homopolymer precursor hydrolyzed using an increase in HCl concentration to 0.10 N but without curing beyond 100  $^{\circ}C$ . The resulting dried film exhibited a 65% degree of siloxane condensation (Figure 7C), a pencil hardness of 6H, and a lateral shrinkage of 40–50%. A dramatic increase in hardness and siloxane condensation is derived from relying more on the chemical cross-linking route (i.e., higher [HCl]), however this comes at the cost of higher shrinkage and associated cracking. Significant discoloration is also observed in these materials if high HCl concentrations are combined with high-temperature curing. For these reasons, it is desirable to minimize the acid content of the films while finding another means to achieve exceptional hardness properties.

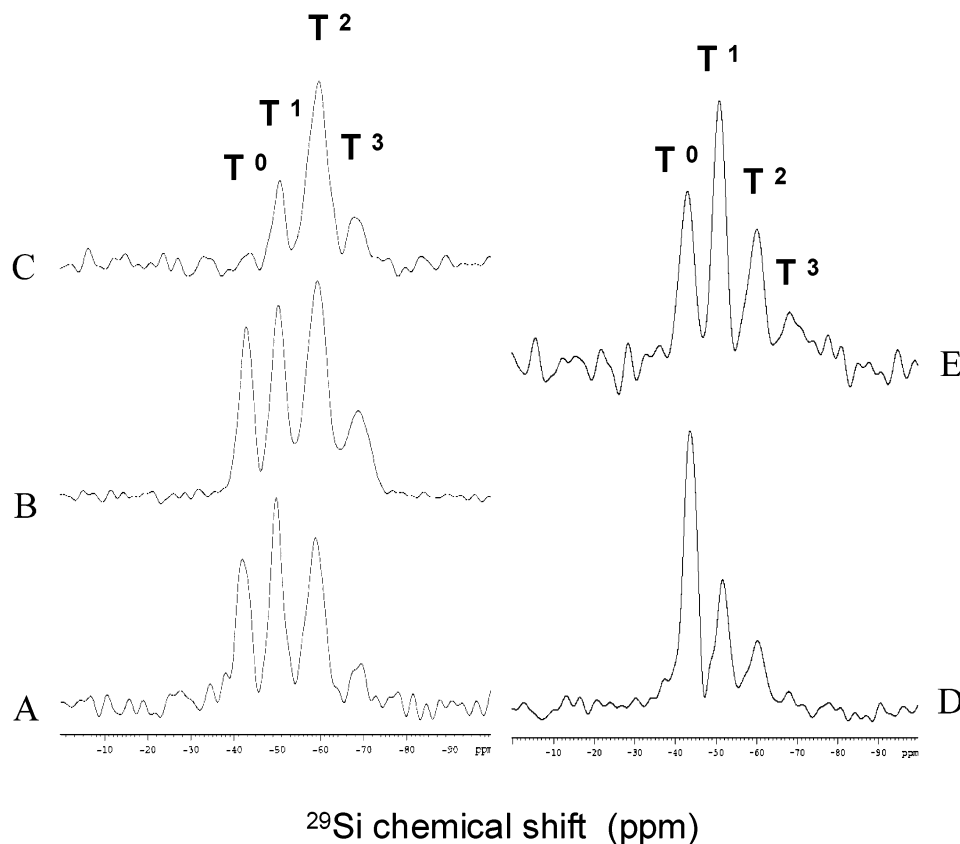


**Figure 7.**  $^{29}\text{Si}$  NMR data for homopolymer (A–C) and 1:4 TMSPM/MMA copolymer (D and E) films representing different chemical and thermal cross-linking treatments. The samples were obtained using the following pairs of acid concentration and cure temperature: (A) 1.7 N, 100 °C; (B) 1.7 N, 150 °C; (C) 1.0 N, 100 °C; (D) 2.0 N, 150 °C; and (E) 2.0 N, 200 °C.

Films made from copolymer precursors exhibited an interesting combination of behaviors. First, a much lower degree of condensative cross-linking is achieved using a similar acid concentration due to the relative dilution of silsesquioxane groups (Figure 7D). Concurrently, higher values of hardness are obtained due to a decrease in the plasticizing effect of the pendant groups (Table 4). As with the homopolymer system, a further increase in the degree of condensation and the hardness is introduced by increasing the temperature of the thermal treatment from 150 to 200 °C (Figure 7E).

The nature of the condensative cross-linking was examined more closely by using DTA characterization of homopolymer films (Figure 8). The location or absence of a glass transition temperature ( $T_g$ —observed as an endothermic shift in the baseline) was used as an indication of the state of cross-linking in the hybrid plastic. It has been shown previously that the  $T_g$  of non-hydrolyzed TMSPM–MMA based copolymers drops below that of PMMA as the content of TMSPM monomer units is increased (poly-MMA,  $T_g = 105$  °C; poly-TMSPM,  $T_g = 48$  °C).<sup>15</sup> This is due to the plasticizing effect of the unreacted pendant groups. The use of 0.020 N HCl and drying at 100 °C results in a film that is sufficiently cross-linked to have a  $T_g$  at around 145 °C (Figure 8A), above that of PMMA. The effect of even a moderate degree of condensation is more than enough to compensate for the plasticizing effect of the pendant groups. Although an increase in HCl concentration to 0.10 N caused a significant increase in the degree of

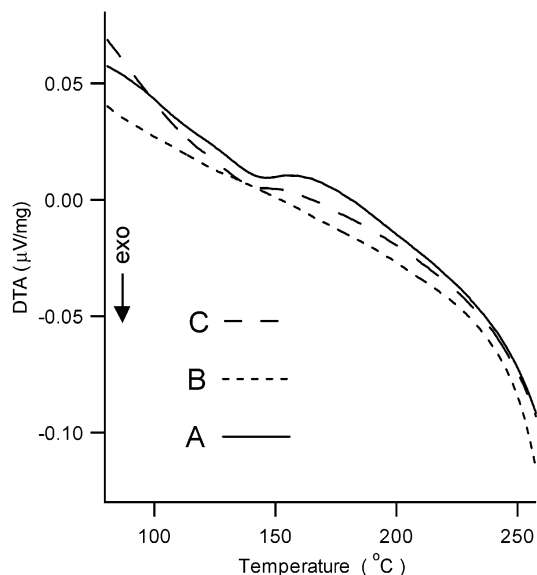


**Figure 8.** DTA data for samples representing thermal and chemical methods of cross-linking polyacrylates containing alkoxy silane pendant groups. The samples were obtained using the following pairs of acid concentration and cure temperature: (A) 1.7 N, 100 °C; (B) 1.7 N, 150 °C; and (C) 1.0 N, 100 °C.

siloxane condensation, it has little effect on the material's resistance to thermal softening (Figure 8C). For this reason, it is expected that the observed siloxane condensation is largely due to intramolecular reaction instead of intermolecular cross-linking that is required for network cross-linking. On the other hand, the film made with a lower acid content and cured to 150 °C

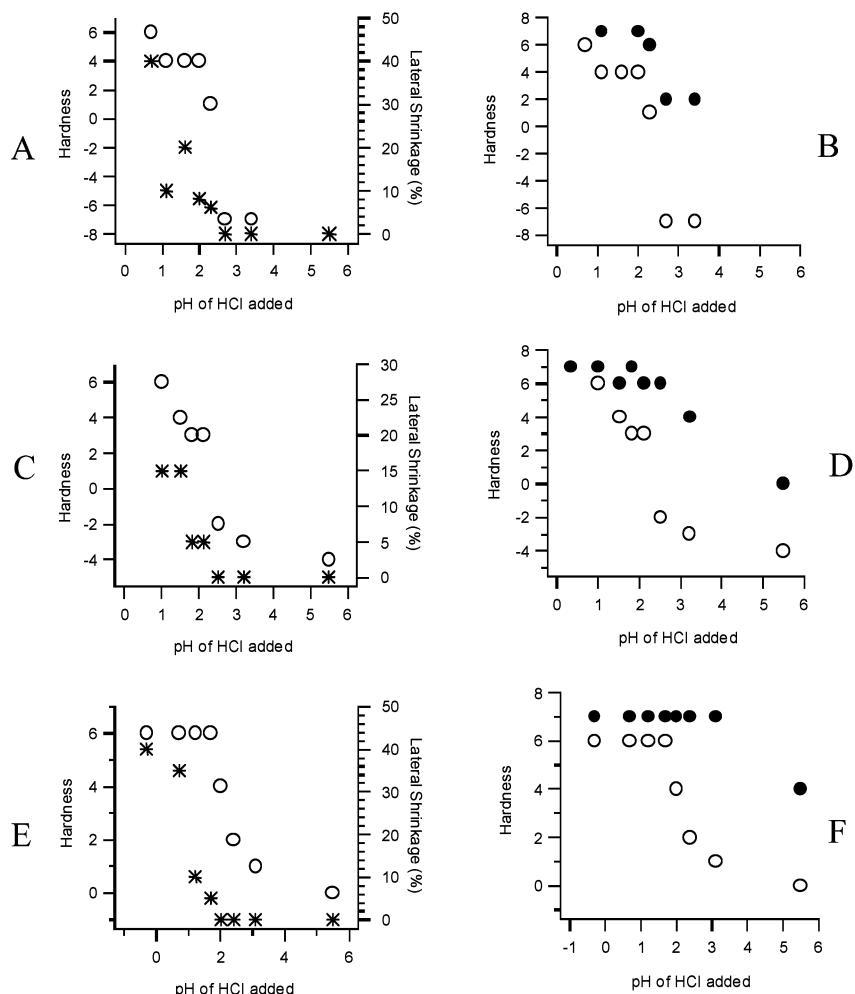


**Figure 9.** Correlation data for pencil hardness, lateral shrinkage, and concentration of acid catalyst for thick films derived from copolymer compositions of 1:1 (A and B), 1:2 (C and D), and 1:4 (E and F) TMSPM/MMA. In plots A, C, and E, the open circles correspond to hardness data of samples cured at 150 °C, and the stars correspond to the shrinkage associated with these cured samples. In plots B, D, and F, the open circles represent samples cured at 150 °C, and the closed circles represent samples cured at 200 °C.

exhibits no evidence of a softening point. These data indicate that thermally induced condensation of a cast film is a particularly effective method of intermolecular cross-linking, even if the hardness of the network is not greatly increased.

A simple model is proposed to explain these seemingly inconsistent phenomena. Because the polymeric film precursors are initially solvated in a nearly random coil conformation ( $a_{MH} = 0.8\text{--}0.9$ , as shown in Table 2), there is more opportunity for intramolecular condensation than for intermolecular condensation (i.e., cross-linking). If the concentration of catalyst is increased then this “non-crosslinking” condensation will predominate prior to the evaporation of the solvent. Once a film is dried, it will have a high degree of condensation and thus be hard, but it will not be highly cross-linked. However, if a lower concentration of catalyst is used, hydrolysis will still occur readily in solution but condensation will not be so rapid. The as-dried film may contain only a slight degree of siloxane condensation, but thermal treatments can then be used to selectively create intermolecular cross-links for thermal stability as well as to increase the hardness. These studies have illustrated that the degree of siloxane condensation may often correlate with hardness but is not an indicator of

overall cross-linking. This relationship depends critically on the cure mechanism used and the structure of the resulting network.

The range of materials properties available from low-acid-content hybrid films was explored further by varying the composition and thermal treatments, and the resulting data are compiled in Figure 9. Film precursors investigated include copolymers having compositions of 1:1 (A, B), 1:2 (C, D), and 1:4 (E, F) TMSPM/MMA. In plots A, C, and E, the open circles correspond to hardness data of samples cured at 150 °C, and the stars correspond to the shrinkage associated with these cured samples. In plots B, D, and F, the open circles represent samples cured at 150 °C, and the closed circles represent samples cured at 200 °C. The most obvious trend is that for all hybrid film compositions the hardness and shrinkage both increase with the acid content used, and all samples exhibit greater hardness by increasing the cure temperature from 150 °C to 200 °C. Furthermore, at higher acid contents and film compositions of 1:2 and 1:4 TMSPM/MMA, the hardness plateaus at values between 6H and 7H. For reference, PMMA and CD-grade polycarbonate have hardnesses of approximately 5H and HB (equal to  $-1$  in Figure 9), respectively. Note that a sudden increase in hardness appears to coincide

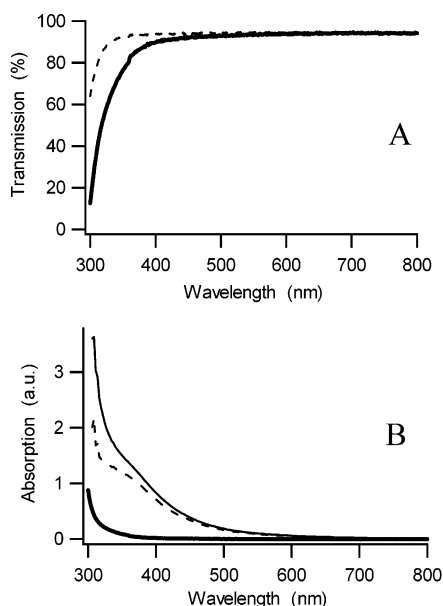


**Figure 10.** (A) UV-vis transmission spectra of a 1:4 TMSPM/MMA copolymer film without HCl after having been dried at 100 °C for 3 h (**bold** trace); the dashed line represents the transmission of the Pyrex dish substrate prior to film casting. (B) UV-vis absorption data from a 1:4 TMSPM/MMA copolymer film without HCl after having been dried at 100 °C for 3 h (**bold** trace) and from the same film after having been cured at 150 °C for 7 h (fine trace); the spectral difference is presented as the dashed line showing an absorption peak at ca. 350 nm that corresponds to a yellow discoloration.

with the isoelectric point of silica (ca. pH 1–2) where hydrolysis rates are at their maximum and condensation rates are at their minimum.

Although films having a hardness of greater than 9H are obtained by using a 1:0 TMSPM/MMA homopolymer and 0.070 N HCl, the shrinkage associated with these materials is extremely high (e.g., 40–50%). Note that the shrinkage data are recorded from relatively thick samples (0.5–1.0 mm) and are expected to be significantly lower for thinner films (e.g., 100–500  $\mu$ m). Thus, compositions producing high-shrinkage, high-hardness, thick films may still be suitable for use as very thin overcoats.

**4. Optical Transparency.** As cast and dried thick films of homopolymer and copolymer exhibit extremely high optical transparency in the visible spectrum (as low as 1% loss/mm at 550 nm, as shown in Figure 10A). However, instances of film discoloration or yellowing (Figure 10B) were consistently observed under specific conditions. Specifically, increases in the HCl content, the cure time and temperature, or the fraction of organic components in the polymer precursor each contribute to the degree of yellowing observed. Infrared spectroscopy of samples before and after thermally induced yellowing reveals the appearance of substituted alkene vibrations (Figure 11), which are consistent with thermal depolymerization of the organic backbone. Neither the HCl content nor the organic content causes noticeable yellowing without heating the material above 100 °C; however, this effect introduces some limits to simultaneously achieving high transparency, high hardness, and low shrinkage in thick films using the present methods.

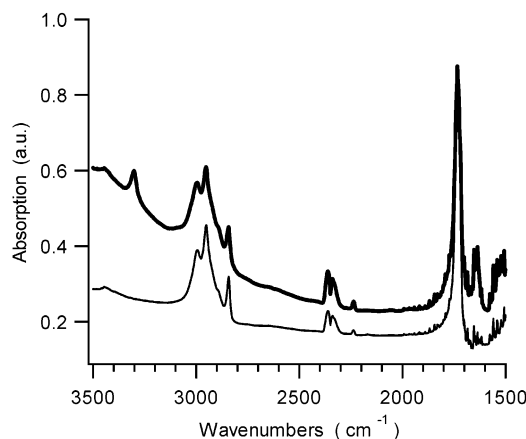


**Figure 11.** Transmission FTIR spectra of 1:4 TMSPM/MMA copolymer films without HCl after having been dried at 100 °C for 3 h (fine trace) and then cured at 150 °C for 11 h (**bold** trace). The vibrational bands at 1640 and 3300 cm<sup>-1</sup> indicate the appearance of substituted alkenes during the curing treatment.

## Discussion

There are several material properties that are desirable in the design of new optical coatings and substrates, including especially the following: hardness, thermomechanical stability, low density, high transparency, and low shrinkage. The studies described herein have identified the relative degrees to which these properties may be achieved in combination by synthesizing silsesquioxane cross-linked PMMA-based hybrid materials. The following discussion will very briefly highlight the observed relationships.

To fabricate TMSPM–MMA copolymer films with optimal hardness, it is necessary to balance several structural characteristics. The first important consideration is the total degree of intermolecular and intramolecular condensation, which contributes inflexible bonding structures such as T<sup>3</sup> Si-groups. The second factor is the polymer composition, which introduces competing effects on the mechanical properties. For example, high ratios of TMSPM/MMA make greater degrees of condensation possible but also disrupt the packing of the acrylic component at low levels of cross-linking. Wei noticed a similar dependency of mechanical properties on the ratio of inorganic to organic content in TMSPM–MMA copolymers, but these studies were focused on materials containing a silicate phase derived from the addition of various relative amounts of TEOS.<sup>12b</sup>

For many relevant technology applications, thermomechanical stability is another important property that can be compared for similar materials by the softening point or  $T_g$ . Unlike the criterion for hardness, the thermomechanical stability is dependent on the degree of cross-linking between polymer chains and not simply on the overall degree of silsesquioxane condensation. The relative degree of intramolecular and intermolecular condensation may be manipulated by varying the emphasis on acid-induced condensation in solution or thermally induced condensation in dried films during processing.

Low-density optical materials are often preferable to heavier materials, especially for monolithic components such as lenses. Lower density is one advantage of



minimizing the inorganic content of a hybrid IPN for a given set of performance requirements. Additional benefits may include higher fracture toughness and better compatibility with optically active organic guest molecules relative to inorganic glasses.

High transparency throughout the visible spectrum is arguably the most important property of an optical coating or substrate material. Light scattering and light absorption are both factors that decrease optical transmission. Light scattering in our system is avoided by the use of a single polymeric precursor that networks to form a single phase. Phase separation between the organic and inorganic phases is prohibited by the covalent propyl-linkages between the polyacrylate and each silane group. Absorption of visible light is not generally a characteristic of alkylsilsesquioxane or poly-(methyl methacrylate); however, yellowing is known to occur if the backbone chain of a polyacrylate is damaged. In the present system, such damage to the acrylic component occurs during heating to 150 °C and higher temperatures and is worsened by a lower ratio of TMSPM/MMA or a higher content of HCl.

The most straightforward means of eliminating or at least minimizing the shrinkage exhibited by a network solid is to eliminate the solvent and other small molecules prior to obtaining a complete percolation of cross-

links.<sup>12e</sup> When available, this strategy has several practical advantages over the extremely creative approach demonstrated by Novak et al.<sup>16</sup> such as the use of less exotic precursors and the presence of covalent linkages between the inorganic and organic phases. Moreover, the production of transparent hybrid IPN materials is extremely difficult without a high concentration of covalent linkages between phases, as it requires a delicate tuning of polymerization rates for each type of network.<sup>7,16a</sup> Regardless of which network is formed first, sequential polymerization<sup>7,8,9,12</sup> and use of covalent coupling between organic and inorganic phases<sup>5</sup> are both critical to the facile creation of high-transparency hybrid IPN materials.

**Acknowledgment.** Funding for this work was provided through the Mitsubishi Chemical Center for Advanced Materials at UCSB. We also especially thank Ted Cais, Karen Frindell, Jianfang Wang, and Ken-ichi Yoshie for their contribution of many valuable discussions.

CM030185J

- 
- (16) (a) Novak, B. M.; Davies, C. *Macromolecules* **1991**, *24*, 5481.  
(b) Ellsworth, M. W.; Novak, B. M. *Chem. Mater.* **1993**, *5*, 839.